Force-distribution sensitivity to cable-tension errors in overconstrained cable-driven parallel robots

Force-Distribution Sensitivity to Cable-Tension Errors in Overconstrained Cable-Driven Parallel Robots[1]

Valentina Mattioni[a], Edoardo Idà[a,*], and Marco Carricato[a]

[a] *Dept. of Industrial Engineering, University of Bologna, 40137 Bologna, Italy*

Abstract

Cable-driven parallel robots (*CDPRs*) employ extendable cables to move their end-effectors (*EEs*) throughout the workspace. Since cables can only sustain tensile stresses, the *EE* is often overconstrained to keep cable tensions within positive limits during motion. In this case, to control the overall cable-tension distribution, one can force-control a particular set of cables, and length-control the others. This work aims at evaluating the maximum value of tension error caused on the length-controlled cables, while force-controlling a chosen cable set, by computing a performance index called *force-distribution sensitivity to cable-tension errors*. This index informs about the maximum expected cable-tension error on the length-controlled cables, if a unitary tension error is committed on a specific set of force-controlled cables, and allows one to determine which set of cables are best to be force-controlled, to ensure the lowest error in the overall tension distribution. The force-distribution sensitivity is derived for a generic overconstrained CDPR, with arbitrary geometry and number of cables. As an application example, its minimum value is computed to characterize the workspace of three exemplifying overconstrained *CDPRs*.

Keywords: Overconstrained robots, cable-driven parallel robots, force distribution, workspace computation, sensitivity analysis.

1. Introduction

Parallel robots usually allow an end-effector (*EE*) to move in space with good performance in terms of dynamics and load capacity, by employing multiple rigid links in a parallel topology. Cable-Driven Parallel Robots (*CDPRs*) replace rigid links with extendable cables. In addition to the benefits provided by the parallel structure, they allow workspace (*WS*) dimensions far greater than standard rigid-link manipulators to be reached. Cables are wound onto actuated drums (*winches*) that can be placed everywhere on the base, and the *EE* is moved around by controlling the cable lengths. The problem of *WS* computation consists in determining if a *EE* pose satisfies a particular criterion, according to the conditions imposed by the

[1] A preliminary version of this paper was presented at the 5th International Conference on Cable-Driven Parallel Robots (CableCon 2021), virtual conference, July 7–9, 2021 [1].

[*] Corresponding author

Email address: edoardo.ida2@unibo.it (Edoardo Idà)

application at hand. For the most part, a pose is considered to belong to the *WS* if the static equilibrium of the platform is satisfied by positive tensions (*wrench closure WS* [2]) or by tensions bounded within known limits (*wrench feasible WS* [3]). An upper limit on cable tensions is usually imposed by the cable's highest load capacity or maximum actuator torque, whereas a lower (positive) limit must be set in order to avoid cable slackness (cables can only pull, but not push). Other criteria concern singularity avoidance [4], cable-cable [5, 6] or cable-platform [7] collision avoidance, just to name a few.

The determination of the robot *WS* is particularly involved for Overconstrained *CDPRs* (*OCDPRs*). The latter have a number of actuated cables higher than the *EE* degrees of freedom (*DoFs*) so that the cables can pull each another. However, constraint redundancy makes the inverse static equilibrium underdetermined (under the assumption that bodies are rigid), namely, an infinite number of cable tensions exist that statically maintain the *EE* in a prescribed configuration. Thus, the *WS* computation for *OCDPRs* mainly consists in determining if a suitable Force Distribution (*FD*), or Tension Distribution (*TD*), exists for a given *EE* pose. It can be crucial in the study of *OCDPRs*, especially for their control, to determine a *FD* which is both optimal according to the application requirements and is continuous along a prescribed trajectory. Many authors treated the problem by minimizing the norm of the cable-tension array [4, 8]. Some of them proposed to optimize other performance indices, such as the largest deviation from the median forces [8]. However, as optimization involves an iterative procedure, it is usually computationally expensive. Thus, several strategies for real-time applications were also proposed, based on a geometric interpretation of the problem equations [9–12].

The computation of a particular *FD* is necessary to introduce an active control in cable tensions, to avoid cable slackness or break while the *EE* is controlled in the desired position. To this end, motor torques are usually given to the system as inputs in order to minimize the position error (output) of the *EE* [13, 14]. In practice, to ensure feasible cable tensions, a *FD* is computed and the torque input is corrected using a specific method, such as a feedback linearization controller [11]. When the *EE* is in contact with the environment, a different strategy is often used [15, 16]. The latter is known as *hybrid position-force* control: the only inputs are the motor angles, but both position and the contact force at the *EE* are the outputs. In [15], the concept of *selection matrix* is introduced to partition the system *DoFs* into position or force-controlled ones. Alternatively, one can define a similar partition but in the internal space of robot coordinates, obtaining a *hybrid force-position control in joint space*. As far as *CDPRs* are concerned, this means that a number of cables, equal to the number of platform *DoFs*, is length-controlled, while the redundant ones are force-controlled, to keep the *EE* in a prescribed configuration while attaining a feasible *FD*. To the authors' knowledge, this simple feedforward control strategy was first hinted at in [17] and [18]. It provides a good *EE* motion accuracy, while it succeeds in maintaining all cables taut throughout the *WS*, without requiring more involved cascade closed-loop controllers [19]. References [17] and [18] suggest no procedure for the selection of the force-controlled cable set, whereas, in the preliminary conference version of this paper [1], this set was determined by computing a novel performance index, the *force-distribution sensitivity to cable-tension error* (or variation), limitedly to a planar *OCDPR* with four cables, one of which is redundant [20].

The main contribution of the current paper is the extension of the *FD* sensitivity to cable-tension errors (formulated in [1] for a planar case with one degree of redundancy) to a more general case, namely for *OCDPRs* with any degree of redundancy and generic spatial architecture, i.e. with arbitrary geometry and number of cables. As application examples, we employ

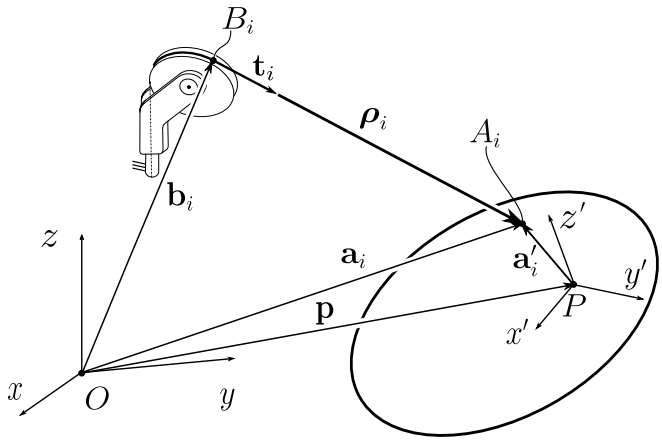

Figure 1: *Geometric model of a cable transmission: $Oxyz$ is an inertial frame; $Px'y'z'$ is a mobile frame attached to the* EE *centre of mass; A_i and B_i are the cable anchor points on the platform and the fixed base, respectively; $\boldsymbol{\rho}_i$ is the i-th cable vector pointing from B_i towards A_i.*

this index to characterise the *WS* of three different *OCDPRs*: a planar manipulator with 5 cables and two spatial manipulators with 7 and 8 cables.

Several other performance indices were proposed in the literature to characterize the performance of *CDPRs* [21, 22]. Some authors introduced performance indices for the analysis of tension sensitivity. For underactuated *CDPRs*, the *maximum tension variation under a cable displacement error* was proposed in order to estimate the geometrico-static performance of the robot [23]. The *Wrench Exertion Capability*, i.e., the maximum wrench that can be exerted in a specific direction within the robot *WS*, was introduced in [24], for all kinds of *CDPRs*. As far as *OCDPRs* are concerned, the *tension factor* was used in [25] and originally proposed in [26], and recently, a force sensitivity based on tension vector and structure matrix was evaluated to ensure a better tension measurement [27]. Unlike the aforementioned indices, the *FD* sensitivity aims at evaluating how the *FD* varies with respect to an error in the tension of a specific set of force-controlled cables, while the remaining ones are length-controlled. This analysis allows one to quantify how much the overall *FD* is influenced by tension errors in the chosen set of force-controlled cables. By evaluating the *FD* sensitivity index for every possible set of force-controlled cables, the set of cables whose tension errors result in the minimum *FD* sensitivity can be identified. In practical terms, this provides a criterion for the selection of force-controlled cables if a hybrid joint-space force-position strategy is employed for the control of an overconstrained *CDPR*. In fact, by choosing the set of cables with the lowest *FD* sensitivity to be force-controlled, the overall *FD* error due to the force-control of a limited set of cables is expected to be the lowest possible. So far, this approach was experimentally validated on a planar prototype and the results are promising [1].

The paper structure is as follows. Section 2 introduces the kinematic model of a generic overconstrained *CDPR*, with an arbitrary degree of redundancy. Section 3 derives the force-distribution sensitivity to cable-tension errors in the most general way. Section 4 proposes the workspace characterisation of three exemplifying *OCDPRs* by way of the proposed index. Finally, in Sec.5 conclusions are drawn and a perspective on future research developments is given.

2. Kinematic Modelling

A *CDPR* consists of a mobile platform (the *EE*) connected to a fixed base by n cables. If n is greater than the *EE DoFs*, n_d, the *CDPR* is overconstrained ($n_d = 3$ or $n_d = 6$, for planar and spatial cases, respectively). The degree of redundancy is defined as $\mu = n - n_d$. According to Fig.1, $Oxyz$ is an inertial frame, whereas $Px'y'z'$ is a mobile frame attached to the *EE* centre of mass. The *EE* pose is described by the position vector $\mathbf{p}$ of P, and a rotation matrix $\mathbf{R}$, which describes the orientation of the mobile platform with respect to the base of the mechanism.

Cables are considered massless and inextensible, assuming that polymer fiber ropes are employed, robot workspace dimension and payload are limited, and cables are under tension. These assumptions are valid for all the examples shown in Sec. 4 and allow for low computational time and complexity, which could become a requirement in real-time applications. Many works experimentally proved that the massless and inextensible model allows one to obtain an acceptable accuracy under the aforementioned assumptions [1, 28–30]. However, the choice of the cable model depends upon the requirements of the desired application, so if those assumptions do not hold true, one can refer to [31, 32] for the most suitable cable models that include cable elasticity and mass and the consequent robot kineto-static model.

Cables are attached to the platform and to the fixed base at points A_i and B_i, respectively, for $i = 1,...,n$. $\mathbf{a}_i$ and $\mathbf{a}'_i$ are the position vectors of A_i with respect to O and P in the inertial frame (Fig.1). The constant position vector of A_i in the mobile frame is denoted by $\mathbf{a}'_{i,P}$. $\mathbf{b}_i$ denotes the position of B_i with respect to O. The latter is a constant vector if the cable exit point is an eyelet, otherwise, it depends on the cable transmission model [33–35], and ultimately the *EE* pose. The i-th cable is modelled as the line segment between points A_i and B_i and, thus, the i-th cable vector can be expressed as [36, 37]:

$$\boldsymbol{\rho}_i = \mathbf{a}_i - \mathbf{b}_i = \mathbf{p} + \mathbf{R}\,\mathbf{a}'_{i,P} - \mathbf{b}_i \tag{1}$$

Considering l_i as the i-th cable length, the constraint imposed by the i-th cable is:

$$\boldsymbol{\rho}_i^T \boldsymbol{\rho}_i - l_i^2 = 0 \tag{2}$$

The unit vector of the i-th cable, pointing from the base towards the platform, is thus:

$$\mathbf{t}_i = \frac{\boldsymbol{\rho}_i}{l_i} \tag{3}$$

3. Force-Distribution Sensitivity

For an *OCDPR* with n cables ($n > n_d$) the *force-distribution (FD) sensitivity* is defined as the maximum tension error obtained in n_d cables, if a unit error (under infinity-norm) is committed in the tensions controlled in the remaining μ cables. In this Section, the *FD* problem is first formulated from the static equilibrium of the platform. Then, the tension array is partitioned by choosing μ cables whose tensions are actively controlled. Finally, the *FD* sensitivity is formulated considering that the μ controlled tensions are the free parameters on which the *FD* depends.

3.1. Force-Distribution problem

The static equilibrium of the platform can be formulated as [36, 37]:

$$\mathbf{J}^T \boldsymbol{\tau} - \mathbf{W} = \mathbf{0} \tag{4}$$

where $\boldsymbol{\tau} \in \mathbb{R}^n$ is the array of cable tensions, $\mathbf{W} \in \mathbb{R}^{n_d}$ is the external wrench acting on the platform, and $\mathbf{J}^T \in \mathbb{R}^{n_d \times n}$, usually referred to as the *structure matrix*, is the transpose of the inverse kinematics Jacobian matrix [4]. The i-th row $\mathbf{J}_i$ of $\mathbf{J}$ is [36]:

$$\mathbf{J}_i = \begin{bmatrix} \mathbf{t}_i{}^T & -\mathbf{t}_i^T \tilde{\mathbf{a}}'_i \end{bmatrix} \tag{5}$$

where the symbol $\sim$ over a vector denotes its skew-symmetric representation.

Due to actuation redundancy, if all bodies are considered as rigid [2], the inverse static problem is underdetermined for an *OCDPR* [38] and it is referred to as *FD* problem. The latter consists in determining a set of cable tensions $\boldsymbol{\tau}$ that is compatible with the *EE* statics in Eq. (4), among the infinitely many possible solutions. The problem may be treated as an optimization problem, where the value of $\boldsymbol{\tau}$ is obtained by optimizing a performance index, according to the application requirements [39]. On the other hand, if a feasible *FD* needs to be computed in real-time for the correct control of the robot, methods with a lower computational effort must be considered. For this purpose, many non-iterative algorithms have been proposed in the literature [8, 10, 40]. However, the problem of optimal *FD* computation will not be discussed in this paper. Indeed, the method here proposed aims at choosing a cable set (among all the cables at disposal) to be force-controlled in order to ensure the lowest tension error in the other length-controlled cables regardless of the actual tension distribution used for controlling the robot.

3.2. Partitioning of the Tension Array

Suitable partitions of the structure matrix and the tension array are now introduced into the static equilibrium equation (4). μ cables are assumed to be force-controlled, and their tensions are denoted by $\boldsymbol{\tau}_c$. The remaining n_d cables are assumed to be position-controlled, and their tensions, $\boldsymbol{\tau}_d$, depend on $\boldsymbol{\tau}_c$, the structure matrix $\mathbf{J}^T$, and the external wrench $\mathbf{W}$. For the sake of simplicity, but without loss of generality, the last μ cables (i.e., the last μ components of $\boldsymbol{\tau}$) are chosen to be force-controlled. Thus, the array $\boldsymbol{\tau}$ of cable tensions may be written as:

$$\boldsymbol{\tau} \triangleq \begin{bmatrix} \boldsymbol{\tau}_d \\ \boldsymbol{\tau}_c \end{bmatrix} \tag{6}$$

and the structure matrix can be partitioned as:

$$\mathbf{J}^T = \begin{bmatrix} \mathbf{J}_d & \mathbf{J}_c \end{bmatrix} \tag{7}$$

where $\mathbf{J}_d \in \mathbb{R}^{n_d \times n_d}$ and $\mathbf{J}_c \in \mathbb{R}^{n_d \times \mu}$. The choice of a different set of force-controlled cables is managed by partitioning $\boldsymbol{\tau}$ and $\mathbf{J}^T$ accordingly, which means that $\mathbf{J}_d$ is formed by the columns of $\mathbf{J}^T$ that will be multiplied with the elements of $\boldsymbol{\tau}_d$, and $\mathbf{J}_c$ by the remaining ones.

[2] This assumption holds for cables only when they are active, namely they are taut.

Introducing definitions (6) and (7) in Eq. (4) yields:

$$\mathbf{W} = \mathbf{J}^T \boldsymbol{\tau} = \begin{bmatrix} \mathbf{J}_d & \mathbf{J}_c \end{bmatrix} \begin{bmatrix} \boldsymbol{\tau}_d \\ \boldsymbol{\tau}_c \end{bmatrix} = \mathbf{J}_d \boldsymbol{\tau}_d + \mathbf{J}_c \boldsymbol{\tau}_c \tag{8}$$

If we additionally decompose $\boldsymbol{\tau}_d$ as $\boldsymbol{\tau}_d = \boldsymbol{\tau}_0 + \Delta\boldsymbol{\tau}$, where $\boldsymbol{\tau}_0$ is the value of $\boldsymbol{\tau}_d$ in case the tension-controlled cables are slack ($\boldsymbol{\tau}_c = 0$), and $\Delta\boldsymbol{\tau}$ is the tension increment due to the actual value of $\boldsymbol{\tau}_c$, $\boldsymbol{\tau}_0$ is defined from the solution of Eq. (8) when $\boldsymbol{\tau}_c = \mathbf{0}$ and $\boldsymbol{\Delta\tau} = \mathbf{0}$, namely:

$$\boldsymbol{\tau}_0 \triangleq \mathbf{J}_d^{-1} \mathbf{W} \tag{9}$$

$\boldsymbol{\tau}_0$ may be computed if $\mathbf{J}_d$ is invertible, that is, the *EE* is not in a geometrically singular configuration. Finally, the expression of $\boldsymbol{\Delta\tau}$ is deduced from Eq. (8), by considering Eq. (9):

$$\boldsymbol{\Delta\tau} = -\mathbf{J}_d^{-1} \mathbf{J}_c \boldsymbol{\tau}_c \tag{10}$$

3.3. Definition of the FD *sensitivity index*

Following the geometrical approach proposed in [39], the force distribution $\boldsymbol{\tau}$ in Eq. (6) can be divided into two terms:

$$\boldsymbol{\tau} = \boldsymbol{\tau}_W + \boldsymbol{\tau}_{ker} \tag{11}$$

where, $\boldsymbol{\tau}_W$ is the solution of Eq. (8) when $\boldsymbol{\tau}_c = \mathbf{0}$ and thus $\boldsymbol{\Delta\tau} = \mathbf{0}$ (see Eq. (9) and (10)), and $\boldsymbol{\tau}_{ker}$ provides a variation of the overall distribution that still satisfies the *EE* equilibrium of Eq. (4). With the definitions given in Eq. (6) and (9), the first contribution of Eq. (11) is expressed as:

$$\boldsymbol{\tau}_W = \begin{bmatrix} \boldsymbol{\tau}_0 \\ \mathbf{0} \end{bmatrix} = \begin{bmatrix} \mathbf{J}_d^{-1} \mathbf{W} \\ \mathbf{0} \end{bmatrix} \tag{12}$$

where $\mathbf{0} \in \mathbb{R}^{\mu \times 1}$. Whereas the contribution $\boldsymbol{\tau}_{ker}$ can be written as:

$$\boldsymbol{\tau}_{ker} = \begin{bmatrix} \boldsymbol{\Delta\tau} \\ \boldsymbol{\tau}_c \end{bmatrix} = \begin{bmatrix} -\mathbf{J}_d^{-1} \mathbf{J}_c \\ \mathbf{I} \end{bmatrix} \boldsymbol{\tau}_c = \mathbf{J}^{\perp} \boldsymbol{\tau}_c, \quad \mathbf{J}^{\perp} \triangleq \begin{bmatrix} -\mathbf{J}_d^{-1} \mathbf{J}_c \\ \mathbf{I} \end{bmatrix} \tag{13}$$

$\mathbf{J}^{\perp} \in \mathbb{R}^{n \times \mu}$ is the right nullspace of the $(n_d \times n)$ matrix $\mathbf{J}^T$, such that $\mathbf{J}^T \mathbf{J}^{\perp} = \mathbf{0} \in \mathbb{R}^{n_d \times \mu}$, and $\mathbf{I}$ is the $(\mu \times \mu)$ identity matrix. Indeed:

$$\mathbf{J}^T \mathbf{J}^{\perp} = \begin{bmatrix} \mathbf{J}_d & \mathbf{J}_c \end{bmatrix} \begin{bmatrix} -\mathbf{J}_d^{-1} \mathbf{J}_c \\ \mathbf{I} \end{bmatrix} = -\mathbf{J}_c + \mathbf{J}_c = \mathbf{0} \tag{14}$$

The introduction of Eqs. (12) and (13) in Eq. (11) yields:

$$\boldsymbol{\tau} = \begin{bmatrix} \mathbf{J}_d^{-1} \mathbf{W} \\ \mathbf{0} \end{bmatrix} + \begin{bmatrix} -\mathbf{J}_d^{-1} \mathbf{J}_c \\ \mathbf{I} \end{bmatrix} \boldsymbol{\tau}_c = \begin{bmatrix} \mathbf{J}_d^{-1} (\mathbf{W} - \mathbf{J}_c \boldsymbol{\tau}_c) \\ \boldsymbol{\tau}_c \end{bmatrix} \tag{15}$$

So, a *FD* can be determined by choosing a particular value for $\boldsymbol{\tau}_c$ and substituting it in Eq. (15).

Considering the definition of the right nullspace $\mathbf{J}^{\perp}$ of the structure matrix (Eq. (13)), for a given set of μ tension-controlled cables, the *force-distribution sensitivity* σ is defined as the maximum tension variation in the position-controlled cables generated by a unit tension variation (or error) of the force-controlled cables, namely:

$$\sigma \triangleq \max_{\|\boldsymbol{\tau}_c\|_\infty = 1} \|\boldsymbol{\Delta\tau}\|_\infty = \| -\mathbf{J}_d^{-1} \mathbf{J}_c \|_\infty \tag{16}$$

Using a double infinity norm for the computation of the *FD* sensitivity is due to the following reasons. First, the infinity norm of $\boldsymbol{\tau}_c$ (for any initial nominal value) allows one to take into account that the tension errors of the force-controlled cables are independent from each other [41]. In addition, the infinity norm of $\boldsymbol{\Delta\tau}$ allows one to identify the maximum tension error value in the position-controlled cables, which will be exploited for the identification of the force-controlled cable set, further on in this Section.

Eq. (16) is valid for a variation $\boldsymbol{\Delta\tau}$ with respect to every nominal value of $\boldsymbol{\tau}_c$, even not equal to zero. In fact, a variation in $\boldsymbol{\tau}_c$ causes a variation in the tension increment $\boldsymbol{\Delta\tau}$ that is independent from the initial value of $\boldsymbol{\tau}_c$. The proof of this statement is provided below, differentiating Eq. (10) with respect to $\boldsymbol{\tau}_c$.

Proof.

$$\frac{\partial \boldsymbol{\Delta\tau}}{\partial \boldsymbol{\tau}_c} = -\frac{\partial(\mathbf{J}_d^{-1}\mathbf{J}_c\boldsymbol{\tau}_c)}{\partial \boldsymbol{\tau}_c} = -\frac{\partial(\mathbf{J}_d^{-1}\mathbf{J}_c)}{\partial \boldsymbol{\tau}_c}\boldsymbol{\tau}_c - \mathbf{J}_d^{-1}\mathbf{J}_c\frac{\partial \boldsymbol{\tau}_c}{\partial \boldsymbol{\tau}_c} \tag{17}$$

Since $\mathbf{J}_d$ and $\mathbf{J}_c$ depend only on the pose

$$\frac{\partial(\mathbf{J}_d^{-1}\mathbf{J}_c)}{\partial \boldsymbol{\tau}_c} = 0 \tag{18}$$

and

$$\frac{\partial \boldsymbol{\tau}_c}{\partial \boldsymbol{\tau}_c} = 1 \tag{19}$$

which yields to:

$$\frac{\partial \boldsymbol{\Delta\tau}}{\partial \boldsymbol{\tau}_c} = -\mathbf{J}_d^{-1}\mathbf{J}_c \tag{20}$$

□

The theoretical minimum value of σ is 0N, which means that for a unit error in the tension of force-controlled cables, no error is propagated in the others. This would be the best scenario, as it would mean that even if the tension values of the position-controlled cables are not monitored, they would not be affected by the force-controlled cables. However, in practical terms, the value $\sigma = 1$N is well accepted, as it means that the manipulator is isotropic with respect to force transmission errors. Namely, the error committed in the force-controlled cables propagates in the remaining cables without being amplified.

3.4. Selection of the force-controlled cable set

For an n-cable manipulator with μ degree of redundancy, different choices of force-controlled cables can be made. The maximum number of possible combinations C is the number of ways of selecting μ cables out of n, without repetition. In terms of a combinatorial problem, this number is expressed as:

$$C = \binom{n}{\mu} = \frac{n!}{(n-\mu)!\mu!} \tag{21}$$

The *FD* sensitivity can be computed for every set of force-controlled cables, thus obtaining C values, $\sigma_1, \ldots, \sigma_C$. After computing all possible C values of the *FD* sensitivity, the minimum value can be identified as:

$$\sigma^\star = \min\{\sigma_1, \ldots, \sigma_C\}. \tag{22}$$

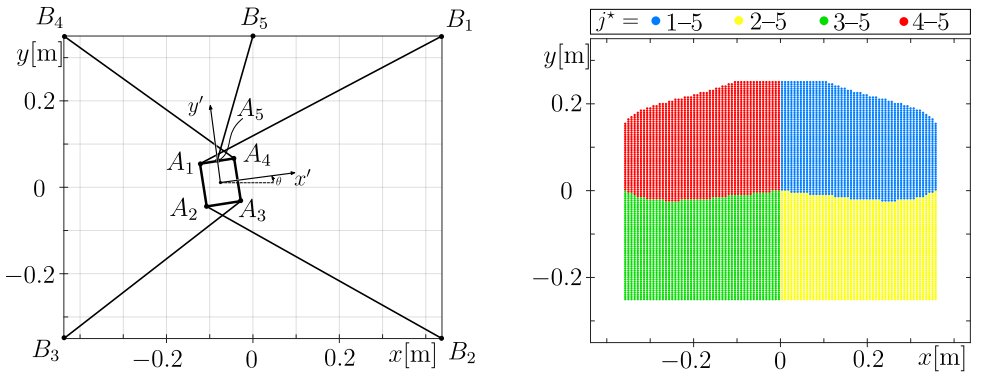

(a) *Robot layout* (b) *Wrench-feasible* WS *with constant* $j^\star$ *areas*

Figure 2: *Characterization of the wrench-feasible constant-orientation* WS *of a planar* 5*-cable* OCDPR *(*$\mu = 2$*) on a regular discrete grid of* $N \times N$ *points (with* $N = 100$*), by means of the minimum-sensitivity index* $\sigma^\star$*:* $j^\star$ *is the cable set that, if force-controlled, propagates the least tension-control errors in the other cables.*

The index $\sigma^\star$ points out which is the cable set that, if force-controlled, propagates the least tension control errors in the other cables. In practical terms, by force-controlling this specific set of cables, denoted by $j^\star$, the minimum cable-tension error with respect to the desired value may be expected. It is worth pointing out that it is possible to compute $\sigma^\star$ in advance, by characterizing the robot *WS*, so that, for every *EE* pose, the set of cables that produces the lowest *FD* sensitivity can be selected to be force-controlled.

4. Workspace characterization

In this Section, the characterization of the constant-orientation wrench-feasible *WS* of some *OCDPRs* is presented as an example of the application of the newly proposed *FD*-sensitivity index. For the sake of brevity, the simple planar 4-cable case (with a degree of redundancy equal to 1) that was illustrated in [1] is not reported here. In the following, instead, we propose three cases that may not be treated with the model presented in [1], but can be analysed with the generalization proposed in this paper: a planar 5-cable *OCDPR* (Sec.4.2), a spatial *OCDPR* with 7 cables (Sec.4.3), and a spatial *OCDPR* with 8 cables (Sec.4.4). The three robots have degrees of redundancy equal to, respectively, 2, 1 and 2. For each case, the minimum-sensitivity index $\sigma^\star$ and the corresponding cable set $j^\star$ are determined in each configuration of the wrench-feasible *WS*. A kernel-based approach is used for the *WS* calculation, where the nullspace (or kernel) $\mathbf{J}^\perp$ is computed as in Eq. (13).

4.1. Wrench Feasibility

The wrench-feasible *WS* is defined as the set of poses for which:

$$\exists \boldsymbol{\tau}: \quad \tau_{min} \preceq \boldsymbol{\tau} \preceq \tau_{max}, \quad \mathbf{J}^T\boldsymbol{\tau} - \mathbf{W} = \mathbf{0} \tag{23}$$

where τ_{min} and τ_{max} are the tension limits, and the symbol $\preceq$ denotes element-wise inequality between a scalar and a vector quantity. Considering the partition (6), Eq. (23) can be written as:

$$\exists \boldsymbol{\tau}_c, \boldsymbol{\tau}_d: \quad \tau_{min} \preceq \boldsymbol{\tau}_c \preceq \tau_{max}, \quad \tau_{min} \preceq \boldsymbol{\tau}_d \preceq \tau_{max}, \quad \mathbf{J}^T\boldsymbol{\tau} - \mathbf{W} = \mathbf{0} \tag{24}$$

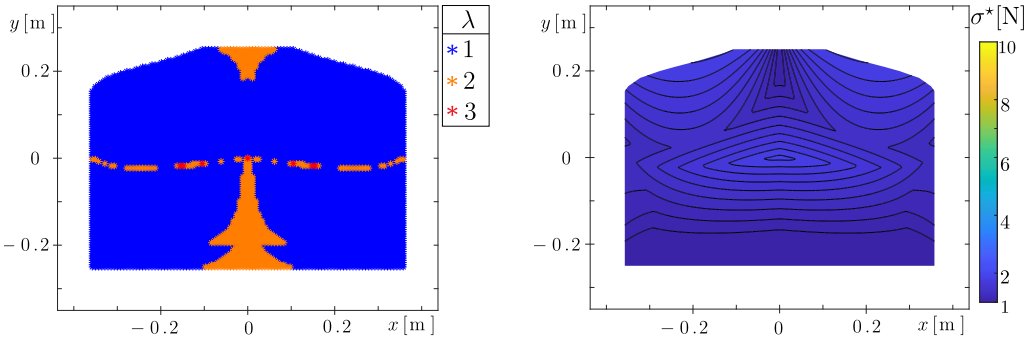

(a) *Multiplicity of solution* (λ) (b) *Variation of the minimum-sensitivity index* ($\sigma^\star$)

Figure 3: *Results of the* FD *sensitivity analysis for the wrench-feasible* WS *of a planar* 5*-cable* OCDPR*: the values of the minimum* FD *sensitivity are computed throughout the* WS*, and the presence of more than one choice for force-controllable cable pair is investigated by computing the multiplicity of solutions for every* WS *configuration.*

Thus, the wrench feasibility condition is verified by checking the existence of a convex region bounded by the inequalities of Eq. (24) [11]. The case $\mu = 1$ results in the search of a scalar interval bounded by $(2 \times n)$ inequalities, as reported in [1]. The case $\mu = 2$ consists in determining a feasible area, namely a convex polytope, and is solved as in [12].

4.2. Planar 5-cable OCDPR

A 5-cable *OCDPR* with a planar architecture (mounted on a vertical plane) is obtained from the 4-cable *OCDPR* with crossed layout considered in [1, 20] by adding one cable on the top of the platform (Fig. 2a). The robot is, therefore, characterised by $\mu = 2$, which means that 2 cables need to be force-controlled in order to apply the hybrid joint-space force-position control strategy. Following Eq. (21), the maximum number of cable pairs is $C = 10$. The *OCDPR* has rectangular base (0.875 m × 0.700 m) and mobile platform (0.080 m × 0.100 m). The inertial frame Oxy is located in the centre of the base and the moving frame $Px'y'$ at the centre of the mobile platform, coinciding with its centre of mass. The following parameters are considered: $m = 2.5$ kg, $\tau_{min} = 10$ N, and $\tau_{max} = 80$ N.

The wrench-feasible *WS* with constant orientation $\mathbf{R} = \mathbf{I}_2$ ($\mathbf{I}_2$ is the identity matrix of order 2) is determined on a regular discrete grid of $N \times N$ points (with $N = 100$). For each *WS* configuration, the minimum *FD* sensitivity $\sigma^\star$ is computed. This index allows us to identify the $j^\star$-th cable pair to be force-controlled among all possible combinations so that the lowest error on the other cable tensions is obtained. The result is represented in Fig. 2b: four distinct constant-$j^\star$ areas emerge from the analysis, which means that, in order to have the lowest error everywhere, it should be necessary to switch the force-controlled cable pair while crossing the border of the areas. In this case, it can be noticed that the 5-th cable is always involved in the $j^\star$ set, which simplifies the switching procedure. As anticipated in [1], computation results show that the configurations near transition borders show very similar values of $\sigma^\star$ in contiguous areas, whereas at the edges of the *WS*, far from the transitions, those values significantly differ. For this reason, once $\sigma^\star$ is determined, the existence of $\sigma_j \leq \gamma\sigma^\star$, with γ slightly bigger than 1, is investigated, and these values are considered equivalent from an engineering

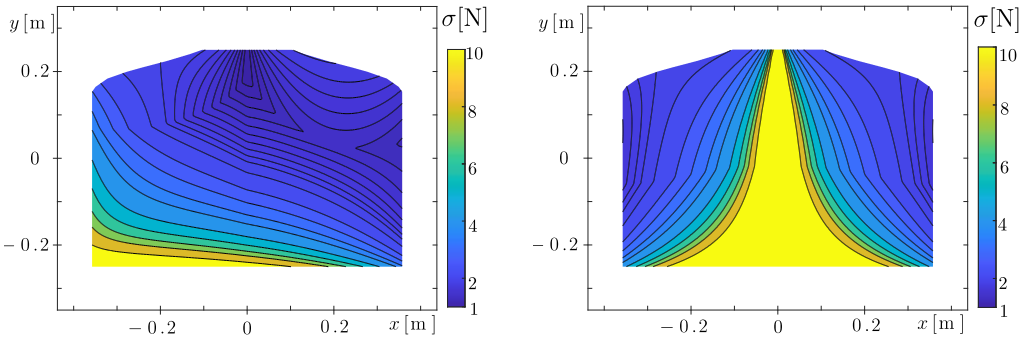

(a) *Values of* FD *sensitivity* σ *while force-controlling cable pair* 1–5

(b) *Values of* FD *sensitivity* σ *while force-controlling cable pair* 1–4

Figure 4: *Variation of the* FD *sensitivity* σ *for different choices of the force-controlled cable pair throughout the wrench-feasible* WS *of a planar* OCDPR *with 5 cables.*

point of view. This allows us to verify the presence of more than one suitable cable pair, called multiplicity λ: if $\lambda = 1$, only one cable pair has $\sigma_j \leq \gamma\sigma^\star$ (the pair $j^\star$); if $\lambda = 2$, two cable pairs have $\sigma_j \leq \gamma\sigma^\star$ ($j^\star$ and another one); and so on. The time needed for the computation of the *WS* points, sensitivity and multiplicity values was 10s on a Windows PC running with an Intel Core i7 CPU at 3.40 GHz, and 16.0 GB RAM. The resulting multiplicity for $\gamma = 1.005$ is shown in Fig. 3a, and it confirms that most of the configurations near transition borders show more than one choice of cable pair since the values of $\sigma^\star$ in contiguous areas are very similar. Indeed, by increasing the tolerance amplitude, the number of configurations characterized by a multiplicity of solutions grows. These results prove that, by considering an appropriate tolerance, the $j^\star$ areas can be enlarged. This might make it possible to work with a constant $j^\star$, thus avoiding the cable-set switching that could cause a discontinuity in the control action [1].

In Fig. 3b the variation of the minimum *FD* sensitivity $\sigma^\star$ throughout the *WS* is shown. Recalling that the value of $\sigma^\star$ is obtained by force-controlling a specific cable set $j^\star$ (Eq. (22)), it can be noticed that, by choosing that set, the minimum *FD* sensitivity is kept close to 1. This value of sensitivity ensures that a low tension error is guaranteed in all cables. It is also interesting to observe how the values of *FD* sensitivity index σ change for different choices of force-controlled cable pairs (σ depends on the force-controlled cable set, see Eq. (16)). For example, by always choosing the pair 1–5 (Fig. 4a), the values of σ are very high in the bottom left corner (up to 10). Whereas they are close to 1 in the top right corner, and there are still good values in the centre *WS*. This result is consistent with Fig. 2b, where the pair $j^\star$ in the top right corner is exactly 1–5. On the contrary, the selection of pair 1–4 gives very high σ values for most of the *WS* configurations (see Fig. 4b), so this pair would be a very inconvenient choice.

In practice, it is possible to switch the force-controlled cables according to the minimum-sensitivity criterion or select the appropriate pair according to the actual *WS* area where the task will be performed. The last solution is certainly the easiest, but it does not ensure the minimum error in cable tensions throughout the whole *WS*.

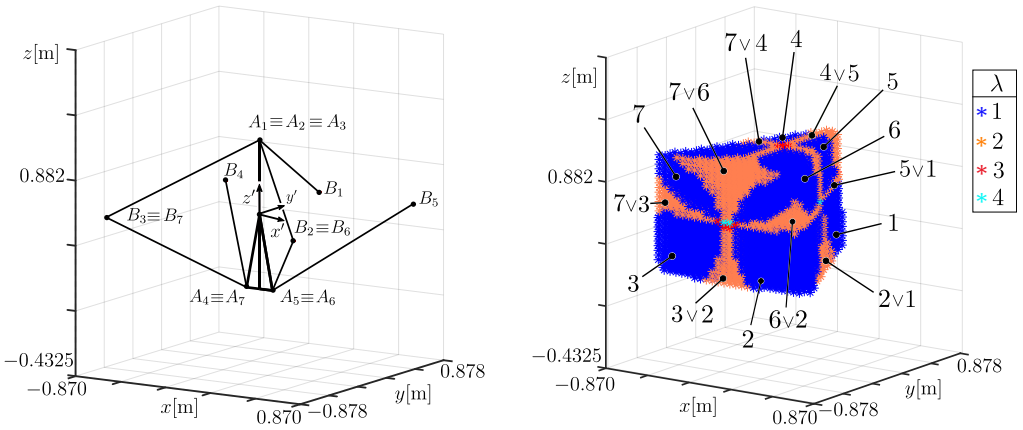

(a) *Robot layout*

(b) *Wrench-feasible* WS *with multiplicity of solution (λ) and constant $j^\star$ areas*

Figure 5: *Characterization of the wrench-feasible constant-orientation* WS *of a spatial* 7*-cable* OCDPR *($\mu = 1$) on a regular discrete grid of $N \times N \times N$ points (with $N = 25$), by means of the minimum-sensitivity index $\sigma^\star$: the values of the minimum* FD *sensitivity are computed throughout the* WS*, and the presence of more than one choice for the force-controllable cable pair is investigated by computing the multiplicity of solutions for every* WS *configuration.*

Table 1: Geometrical properties of the 7-cable *OCDPR*.

i	1	2	3	4	5	6	7
$\mathbf{b}_i$ [m]	$\begin{bmatrix} 0 \\ 0.725 \\ 0.625 \end{bmatrix}$	$\begin{bmatrix} 0.725 \\ -0.725 \\ 0.625 \end{bmatrix}$	$\begin{bmatrix} -0.725 \\ -0.725 \\ 0.625 \end{bmatrix}$	$\begin{bmatrix} -0.725 \\ 0.725 \\ 0.625 \end{bmatrix}$	$\begin{bmatrix} 0.725 \\ 0.725 \\ 0.625 \end{bmatrix}$	$\begin{bmatrix} 0.725 \\ -0.725 \\ 0.625 \end{bmatrix}$	$\begin{bmatrix} -0.725 \\ -0.725 \\ 0.625 \end{bmatrix}$
$\mathbf{a}'_i$ [m]	$\begin{bmatrix} 0 \\ 0 \\ 0.500 \end{bmatrix}$	$\begin{bmatrix} 0 \\ 0 \\ 0.500 \end{bmatrix}$	$\begin{bmatrix} 0 \\ 0 \\ 0.500 \end{bmatrix}$	$\begin{bmatrix} -0.100 \\ 0 \\ -0.500 \end{bmatrix}$	$\begin{bmatrix} 0.100 \\ 0 \\ -0.500 \end{bmatrix}$	$\begin{bmatrix} 0.100 \\ 0 \\ -0.500 \end{bmatrix}$	$\begin{bmatrix} -0.100 \\ 0 \\ -0.500 \end{bmatrix}$

4.3. Spatial 7-cable OCDPR

The structure of the 7-cable *OCDPRs* (Fig.5a) is taken from the well-known robot *FALCON-7* [42]. The geometrical properties of the robot are summarised in Tab. 1. The inertial frame $Oxyz$ is located in the centre of the base and the moving frame $Px'y'z'$ at the centre of the mobile platform, coinciding with its centre of mass. The only external load applied to the robot *EE* is gravity, and its mass is assumed to be $m = 1$ kg. Tension limits are set to $\tau_{min} = 50$ N, and $\tau_{max} = 5000$ N. The robot has one degree of redundancy ($\mu = 1$), thus, considering the hybrid joint-space force-position control strategy, one cable may be force-controlled, whereas the others are length-controlled. Following Eq. (21), the number of possible cable combinations is $C = 7$.

The wrench-feasible *WS* with constant orientation $\mathbf{R} = \mathbf{I}_3$ ($\mathbf{I}_3$ is the identity matrix of order 3) is determined on a regular discrete grid of $N \times N \times N$ points (with $N = 25$). For each *WS* configuration, the minimum *FD* sensitivity $\sigma^\star$ is computed. The multiplicity of cable sets

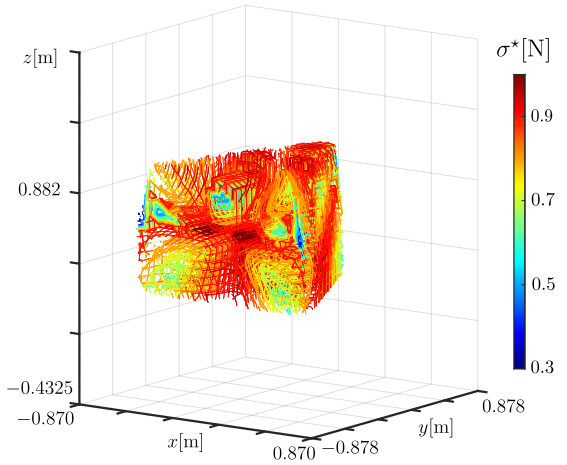

Figure 6: *Variation of the minimum sensitivity $\sigma^\star$ throughout the wrench-feasible* WS *of a spatial* OCDPR *with 7 cables: $\sigma^\star$ approaches* 1N *in the zones where the multiplicity of solutions λ is greater than* 1 *(Fig. 5b).*

that give the minimum value of sensitivity for a tolerance $\gamma = 1.05$ is also calculated. The time needed for the computation of the *WS* points, sensitivity and multiplicity values was 5s on a Windows PC running with an Intel Core i7 CPU at 3.40 GHz, and 16.0 GB RAM. Results are shown in Fig. 5b. Even in this case, most of the configurations near the transition borders (orange, red and cyan zones) show more than one optimal choice for the force-controlled cable, as the values of $\sigma^\star$ in contiguous areas are very similar. Fig. 5b also reports the cable with the smallest sensitivity in each area. The blue region identifies the presence of one suitable choice for the force-controlled cable, while the orange region corresponds to two suitable choices. In the red areas, three choices are available. In the cyan zone, at the centre of the foreground side of the *WS*, four different cables (2, 3, 6, and 7) can be chosen.

Moreover, the study of the actual value of the minimum sensitivity $\sigma^\star$ can be helpful for the estimation of the tension error throughout the *WS*. Fig. 6 shows the variation of the minimum sensitivity throughout the *WS* in 3-D. The range of values resulting from the analysis is between $\sigma^\star = 0.3$ N and $\sigma^\star = 1$ N. It is worth noting that the $\sigma^\star$ value is less than 1N (which means a low propagation of tension error in the length-controlled cables), while it approaches 1N in a few zones, exactly where $\lambda > 1$. This means that working in a region with multiplicity close to/equal to 1 ensures low tension errors in the *FD*. To verify this observation, some cross sections of the *WS* are displayed in Fig. 7. Figures 7a,7b and 7c show cross sections for $x = -0.3$m, $x = -0.2$m and $x = 0$m, respectively. Sections for positive values of x are omitted, as the *WS* is symmetric with respect to yz plane. Figures 7d,7e and 7f show cross sections for $y = -0.5$m, $y = -0$m and $y = 0.3$m. In this case, sections for both positive and negative values of y are considered, as there is no *WS* symmetry. Finally, cross sections for $z = 0.4$m, $z = 0.6$m and $z = 0.8$m are shown in Fig. 7g,7h and 7i. Only positive values are considered thanks to the symmetry of the *WS* with respect to xy plane.

These graphs show that, for the most part of the *WS*, the value of the *FD* sensitivity is less than 1. In some sections (e.g., Fig.7c, and Fig.7i), it can be noticed that the unit-sensitivity areas are small. This means that, in the worst-case scenario, a unit error in the force-controlled cables results in a unit error in the other cables. That is, the manipulator is roughly isotropic

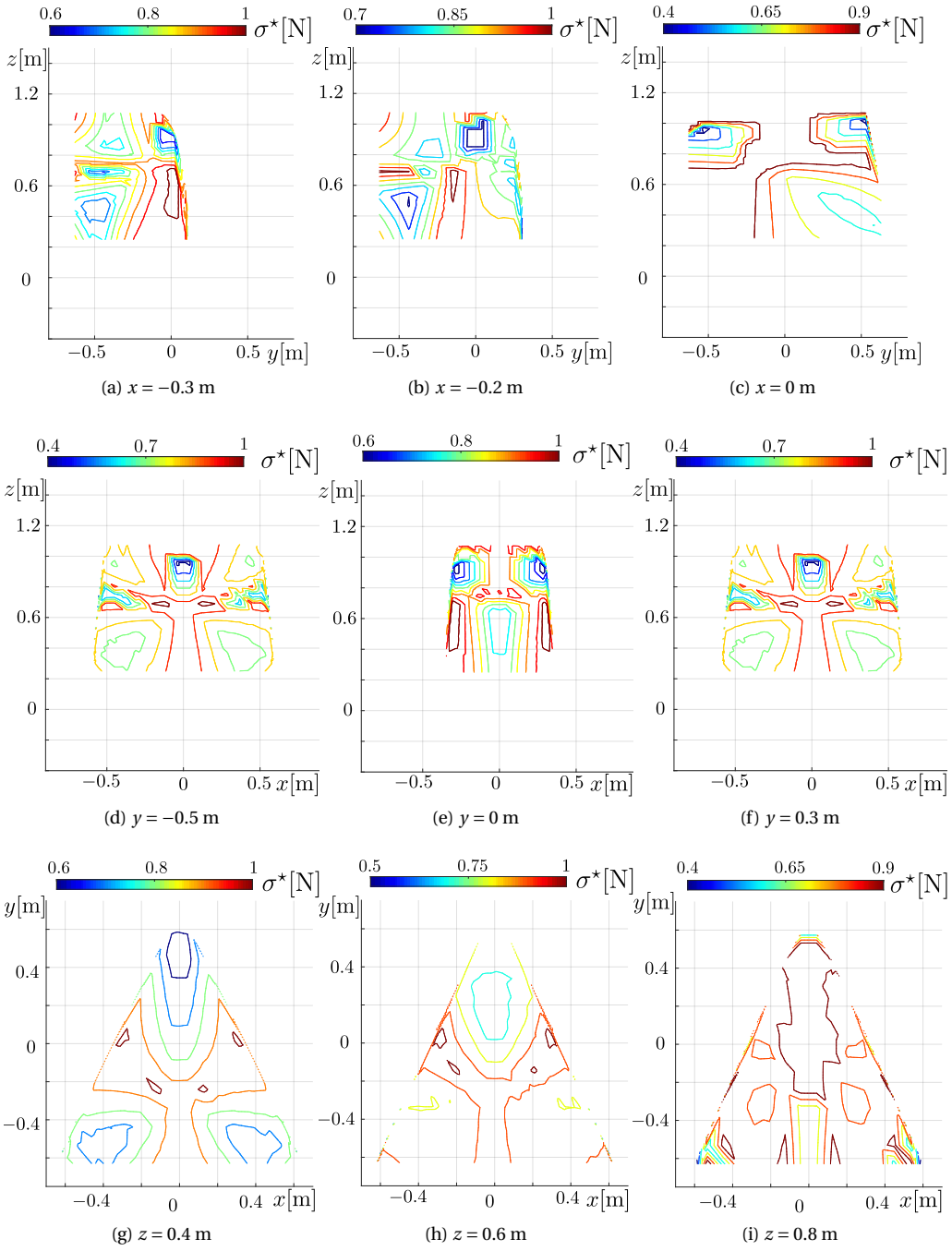

Figure 7: *Variation of the minimum* FD *sensitivity* $\sigma^\star$ *for different cross sections of the* 7*-cable robot* WS *(Fig. 6). The value of* $\sigma^\star$ *is mostly close to* 1N*, even in the innermost regions of the* WS.

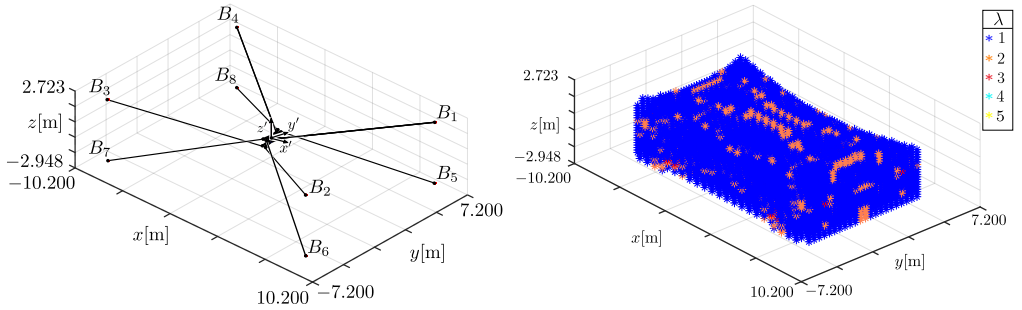

(a) *Robot layout*

(b) *Wrench-feasible* WS *with Wrench-feasible* WS *with multiplicity of solution* (λ)

Figure 8: *Characterization of the wrench-feasible constant-orientation* WS *of a spatial* 8*-cable* OCDPR ($\mu = 2$) *by means of the minimum-sensitivity index* $\sigma^\star$*: the values of the minimum* FD *sensitivity are computed throughout the* WS*, and the presence of more than one choice for the force-controllable cable pair is investigated by computing the multiplicity of solutions for every* WS *configuration.*

Table 2: Geometrical properties of the 8-cable *OCDPR*.

i	1	2	3	4	5	6	7	8
$\mathbf{b}_i$ [m]	$\begin{bmatrix} 8.500 \\ 6.000 \\ 2.250 \end{bmatrix}$	$\begin{bmatrix} 8.500 \\ -6.000 \\ 2.250 \end{bmatrix}$	$\begin{bmatrix} -8.500 \\ -6.000 \\ 2.250 \end{bmatrix}$	$\begin{bmatrix} -8.500 \\ 6.000 \\ 2.250 \end{bmatrix}$	$\begin{bmatrix} 8.500 \\ 6.000 \\ -2.250 \end{bmatrix}$	$\begin{bmatrix} 8.500 \\ -6.000 \\ -2.250 \end{bmatrix}$	$\begin{bmatrix} -8.500 \\ -6.000 \\ -2.250 \end{bmatrix}$	$\begin{bmatrix} -8.500 \\ 6.000 \\ -2.250 \end{bmatrix}$
$\mathbf{a}'_i$ [m]	$\begin{bmatrix} 0.113 \\ 0.750 \\ -0.250 \end{bmatrix}$	$\begin{bmatrix} 0.113 \\ -0.750 \\ -0.250 \end{bmatrix}$	$\begin{bmatrix} -0.113 \\ -0.750 \\ -0.250 \end{bmatrix}$	$\begin{bmatrix} -0.113 \\ 0.750 \\ -0.250 \end{bmatrix}$	$\begin{bmatrix} 0.113 \\ 0.750 \\ 0.250 \end{bmatrix}$	$\begin{bmatrix} 0.113 \\ -0.750 \\ 0.250 \end{bmatrix}$	$\begin{bmatrix} -0.113 \\ -0.750 \\ 0.250 \end{bmatrix}$	$\begin{bmatrix} -0.113 \\ 0.750 \\ 0.250 \end{bmatrix}$

with respect to tension error propagation if the optimal cable is chosen to be force-controlled. If not, the error would be amplified, and the result would be similar to that of Fig. 4b, discussed in Sec. 4.2.

4.4. Spatial 8-cable OCDPR

The considered 8-cable *OCDPR* (Fig.8a) presents the architecture of the *IPAnema3* robot [36]. The geometrical properties of the robot are summarised in Tab. 2. The inertial frame $Oxyz$ is located in the centre of the base and the moving frame $Px'y'z'$ at the centre of the mobile platform, coinciding with its centre of mass. The only external load applied to the robot *EE* is gravity, and its mass is assumed to be $m = 50$kg. Tension limits are set to $\tau_{min} = 50$ N, and $\tau_{max} = 2000$ N. The robot has two degrees of redundancy ($\mu = 2$), thus, 2 cables have to be force-controlled, whereas the others may be length-controlled. The number of possible cable pairs is $C = 28$ (see Eq. (21)). The wrench-feasible *WS* with the constant orientation $\mathbf{R} = \mathbf{I}_3$ is determined and, for each *WS* configuration, the minimum *FD* sensitivity $\sigma^\star$ is computed. The multiplicity for $\gamma = 1.05$ is investigated, and shown in Fig. 8b. The time needed for the computation of the *WS* points, sensitivity and multiplicity values was 26s on a Windows PC running with an Intel Core i7 CPU at 3.40 GHz, and 16.0 GB RAM. The multiplicity reaches the value $\lambda = 5$, but both this value and $\lambda = 4$ are not visible from the chosen *WS* view. This means that in those areas the same value of $\sigma^\star$ is obtained with up to 5 different force-controlled

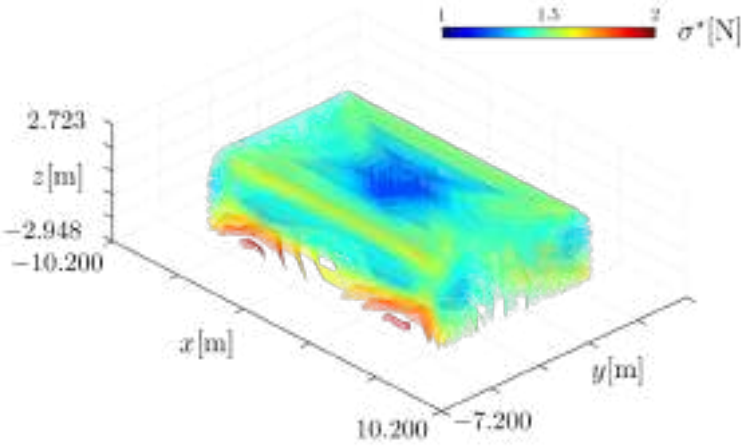

Figure 9: *Variation of the minimum sensitivity $\sigma^\star$ throughout the wrench-feasible* WS *of a spatial* OCDPR *with 8 cables: $\sigma^\star$ is roughly* 1N *in the inner zones, whereas it approaches* 2N *near the* WS *borders.*

cable sets. Since there are up to 28 distinct constant-$j^\star$ areas, they can not be pointed out in this figure. However, the presence of wider blue areas ($\lambda = 1$) separated by thinner orange zones ($\lambda = 2$) can be noticed.

The value of the minimum sensitivity $\sigma^\star$ is studied in order to estimate the tension error throughout the *WS*. Fig. 9 shows the variation of the minimum sensitivity throughout the *WS* in 3-D. The range of values resulting from the analysis is between $\sigma^\star = 1$ N and $\sigma^\star = 2$ N. A value of $\sigma^\star$ equal to 2 N means doubling the error in the length-controlled cables, which would be an undesirable situation. Thus, in order to verify the presence of other zones with $\sigma^\star = 2$ N, some cross sections of the robot *WS* are displayed in Fig. 10. Figures 10a,10b and 10c show cross sections for $x = -5$m, $x = -2$m and $x = 0$m, rispectively. Figures 10d,10e and 10f show cross sections for $y = -4$m, $y = -2.5$m and $y = 0$m. Sections for positive values of x and y are omitted, as the *WS* is symmetric with respect to yz and xz plane. Finally, cross sections for $z = -1.5$m, $z = 0$m and $z = 1.5$m are shown in Fig. 10g,10h and 10i. These graphs show that the value of *FD* sensitivity is almost unitary in the centre workspace (see Fig. 10c, 10f and 10h), whereas its value increases near the *WS* borders (see Fig. 10a, 10e and 10i). This fact suggests that working in the outermost *WS* regions with this *CDPR* layout would be risky.

5. Conclusions and outlook

In this paper, a new performance index, called force-distribution (*FD*) sensitivity to cable tension error (or variation) was presented for overconstrained *CDPRs* with arbitrary (spatial or planar) geometry and arbitrary degree of redundancy. In case a hybrid joint-space force-position strategy is applied for the control of the *OCDPR*, the *FD* sensitivity allows one to evaluate the maximum expected cable tension error on the length-controlled cables if a unitary tension error (in the infinity-norm sense) is committed on the force-controlled cables. The *FD* sensitivity was investigated for all possible combinations of force-controlled cables, and, then, its minimum value was identified. This value corresponds to the set of cables that need to be force-controlled to ensure the lowest error in the overall *FD*. As an application example, the wrench-feasible workspace of three overconstrained *CDPRs* was investigated: a planar

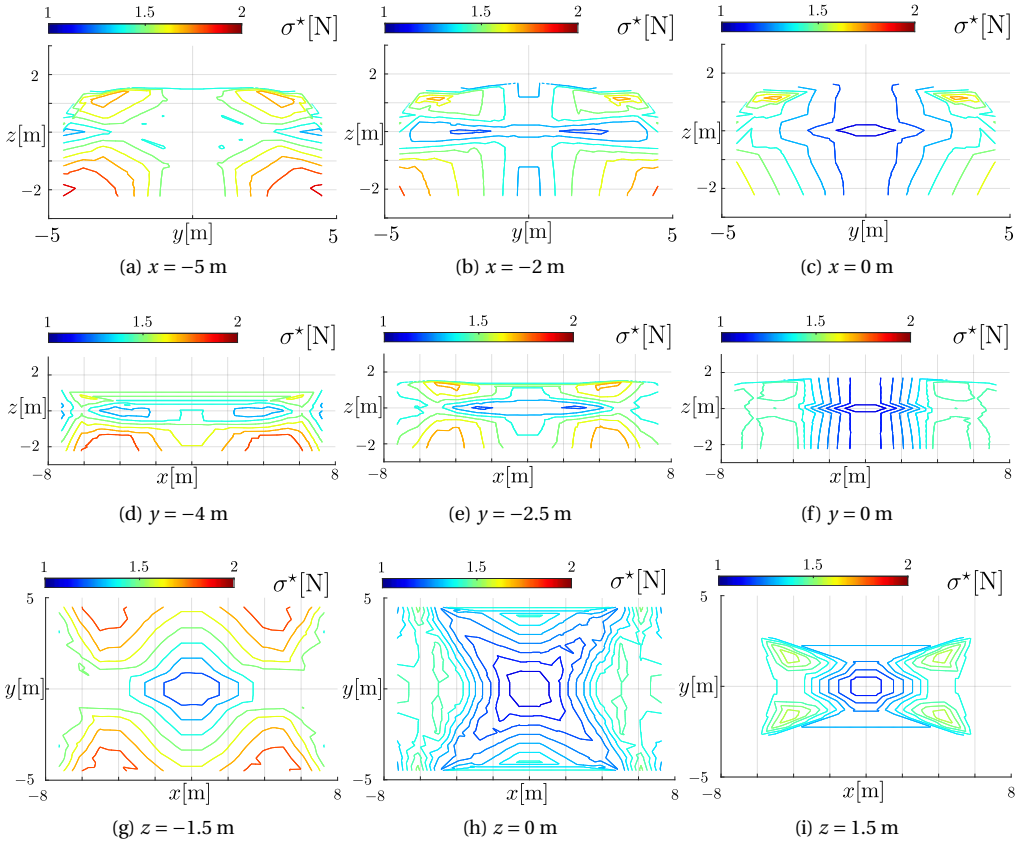

(a) $x = -5$ m (b) $x = -2$ m (c) $x = 0$ m

(d) $y = -4$ m (e) $y = -2.5$ m (f) $y = 0$ m

(g) $z = -1.5$ m (h) $z = 0$ m (i) $z = 1.5$ m

Figure 10: *Variation of the minimum* FD *sensitivity* $\sigma^\star$ *for different cross sections of the* 8*-cable robot* WS *(Fig. 9). These sections confirm that the value of* $\sigma^\star$ *is mostly around* 1N *in the inner region of the* WS.

manipulator with 5 cables and two spatial manipulators with 7 and 8 cables. Their *FD* sensitivity was computed for each *WS* configuration and for each possible set of force-controllable cables. The minimum value of the index was determined, and the variation of the minimum *FD* sensitivity throughout the workspace was presented.

The performed analysis provides interesting results: if a random set of cables is force-controlled, the tension error in that set is amplified in the position-controlled cables in many *WS* zones. On the contrary, if the optimal set of cables, which corresponds to the minimum value of *FD* sensitivity, is force-controlled, the tension error is kept small for almost the whole *WS*. These results proved that the *FD* sensitivity index provides a valuable criterion for the selection of the force-controlled cable set when a hybrid force-position control strategy in joint space is adopted for a *OCDPR* with any degree of redundancy.

Future works include the experimental validation of this approach on a *OCDPR* with a degree of redundancy greater than 1. Promising results are expected, considering that, in the previous conference version of this paper [1], the application of this approach to a planar 4-cable *CDPR* experimentally proved that all cables were kept taut during motion even near the workspace borders.

In addition, the influence of other relevant variables, such as *EE* mass and cable anchor points position, on the *FD* sensitivity index will be investigated, in order to make the proposed approach more robust. From a practical viewpoint, it would also be interesting to consider the selection of position-controlled cables that minimize the position error. Analysing both minimization of positioning errors and force-distribution errors could lead to the optimal choice of cable decomposition.

Finally, we will study the problem concerning the stability of the hybrid position-force controller in case the force-controlled cable set is switched in real time, during the execution of a trajectory.

References

[1] V. Mattioni, E. Idà, M. Carricato, Force-distribution sensitivity to cable-tension errors: A preliminary investigation, in: M. Gouttefarde, T. Bruckmann, A. Pott (Eds.), Cable-Driven Parallel Robots, Springer International Publishing, Cham, 2021, pp. 129–141.

[2] M. Gouttefarde, C. M. Gosselin, Analysis of the wrench-closure workspace of planar parallel cable-driven mechanisms, IEEE Transactions on Robotics 22 (3) (2006) 434–445.

[3] M. Gouttefarde, D. Daney, J.-P. Merlet, Interval-analysis-based determination of the wrench-feasible workspace of parallel cable-driven robots, IEEE Transactions on Robotics 27 (1) (2011) 1–13.

[4] M. Hiller, S. Fang, S. Mielczarek, R. Verhoeven, D. Franitza, Design, analysis and realization of tendon-based parallel manipulators, Mechanism and Machine Theory 40 (4) (2005) 429 – 445.

[5] S. Perreault, P. Cardou, C. M. Gosselin, M. J.-D. Otis, Geometric determination of the interference-free constant-orientation workspace of parallel cable-driven mechanisms, ASME J. Mechanisms Robotics 2 (3) (2010) 031016.

[6] K. Youssef, M. J.-D. Otis, Reconfigurable fully constrained cable driven parallel mechanism for avoiding interference between cables, Mechanism and Machine Theory 148 (2020) 103781.

[7] P. Tempel, F. Schnelle, A. Pott, P. Eberhard, Design and programming for cable-driven parallel robots in the german pavilion at the expo 2015, Machines 3 (3) (2015) 223–241.

[8] C. Gosselin, M. Grenier, On the determination of the force distribution in overconstrained cable-driven parallel mechanisms, Meccanica 46 (1) (2011) 3–15.

[9] K. Müller, C. Reichert, T. Bruckmann, Analysis of a real-time capable cable force computation method, in: A. Pott, T. Bruckmann (Eds.), Cable-Driven Parallel Robots, Springer International Publishing, Cham, 2015, pp. 227–238.

[10] A. Pott, An improved force distribution algorithm for over-constrained cable-driven parallel robots, in: F. Thomas, A. Perez Gracia (Eds.), Computational Kinematics, Springer Netherlands, Dordrecht, 2014, pp. 139–146.

[11] S.-R. Oh, S. K. Agrawal, Cable suspended planar robots with redundant cables: Controllers with positive tensions, IEEE Transactions on Robotics 21 (3) (2005) 457–465.

[12] M. Gouttefarde, J. Lamaury, C. Reichert, T. Bruckmann, A versatile tension distribution algorithm for n -dof parallel robots driven by $n+2$ cables, IEEE Transactions on Robotics 31 (6) (2015) 1444–1457.

[13] S. Fang, D. Franitza, M. Torlo, F. Bekes, M. Hiller, Motion control of a tendon-based parallel manipulator using optimal tension distribution, IEEE/ASME Transaction on Mechatronics 9 (3) (2004) 561–568.

[14] X. Wang, S. Ma, Q. Lin, Hybrid pose/tension control based on stiffness optimization of cable-driven parallel mechanism in wind tunnel test, in: 2nd International Conference on Control, Automation and Robotics (ICCAR), 2016, pp. 75–79.

[15] J. Jun, X. Jin, A. Pott, S. Park, J.-O. Park, S. Y. Ko, Hybrid position/force control using an admittance control scheme in cartesian space for a 3-dof planar cable-driven parallel robot, International Journal of Control, Automation and Systems 14 (4) (2016) 1106–1113.

[16] W. Kraus, P. Miermeister, V. Schmidt, A. Pott, Hybrid position-force control of a cable-driven parallel robot with experimental evaluation, Mechanical Sciences 6 (2) (2015) 119–125.

[17] S. Bouchard, C. Gosselin, A simple control strategy for overconstrained parallel cable mechanisms, in: Proc. of the 20th Canadian Congress of Applied Mechanics (CANCAM 2005), Montreal, Quebec, Canada, 2005.

[18] T. Bruckmann, L. Mikelsons, M. Hiller, D. Schramm, A new force calculation algorithm for tendon-based parallel manipulators, in: 2007 IEEE/ASME int. conf. on advanced intelligent mechatronics, Zurich, Switzerland, 2007, pp. 1–6.

[19] W. Kraus, V. Schmidt, P. Rajendra, A. Pott, System identification and cable force control for a cable-driven parallel robot with industrial servo drives, in: 2014 IEEE International Conference on Robotics and Automation (ICRA), 2014, pp. 5921–5926.
[20] V. Mattioni, E. Ida', M. Carricato, Design of a planar cable-driven parallel robot for non-contact tasks, Applied Sciences 11 (20) (2021) 9491.
[21] E. Idà, D. Marian, M. Carricato, A deployable cable-driven parallel robot with large rotational capabilities for laser-scanning applications, IEEE Robotics and Automation Letters 5 (3) (2020) 4140–4147.
[22] G. Mottola, C. Gosselin, M. Carricato, Effect of actuation errors on a purely-translational spatial cable-driven parallel robot, in: 2019 IEEE 9th Annual International Conference on CYBER Technology in Automation, Control, and Intelligent Systems (CYBER), 2019, pp. 701–707.
[23] E. Idà, M. Carricato, A new performance index for underactuated cable-driven parallel robots, in: M. Gouttefarde, T. Bruckmann, A. Pott (Eds.), Cable-Driven Parallel Robots, Springer International Publishing, Cham, 2021, pp. 24–36.
[24] G. Boschetti, A. Trevisani, Cable robot performance evaluation by wrench exertion capability, Robotics 7 (2) (2018) 15.
[25] C. B. Pham, S. H. Yeo, G. Yang, I.-M. Chen, Workspace analysis of fully restrained cable-driven manipulators, Robotics and Autonomous Systems 57 (9) (2009) 901–912.
[26] R. Verhoeven, M. Hiller, Tension distribution in tendon-based stewart platforms, in: J. Lennarčič, F. Thomas (Eds.), Advances in Robot Kinematics, Springer Netherlands, Dordrecht, 2002, pp. 117–124.
[27] Q. Chen, Q. Lin, G. Wei, L. Ren, Tension vector and structure matrix associated force sensitivity of a 6-dof cable-driven parallel robot, Proceedings of the Institution of Mechanical Engineers, Part C: Journal of Mechanical Engineering Science 0 (0) (2021) 09544062211026344.
[28] E. Idà, S. Briot, M. Carricato, Identification of the inertial parameters of underactuated cable-driven parallel robots, Mechanism and Machine Theory 167 (2022) 104504.
[29] C. Gosselin, Global Planning of Dynamically Feasible Trajectories for Three-DOF Spatial Cable-Suspended Parallel Robots, Springer Berlin Heidelberg, Berlin, Heidelberg, 2013, pp. 3–22.
[30] R. Chellal, E. Laroche, L. Cuvillon, J. Gangloff, An Identification Methodology for 6-DoF Cable-Driven Parallel Robots Parameters Application to the INCA 6D Robot, Springer Berlin Heidelberg, Berlin, Heidelberg, 2013, pp. 301–317.
[31] I. Chawla, P. Pathak, L. Notash, A. Samantaray, Q. Li, U. Sharma, Effect of selection criterion on the kineto-static solution of a redundant cable-driven parallel robot considering cable mass and elasticity, Mechanism and Machine Theory 156 (2021) 104175.
[32] E. Ottaviano, A. Arena, V. Gattulli, Geometrically exact three-dimensional modeling of cable-driven parallel manipulators for end-effector positioning, Mechanism and Machine Theory 155 (2021) 104102.
[33] E. Idá, J.-P. Merlet, M. Carricato, Automatic self-calibration of suspended under-actuated cable-driven parallel robot using incremental measurements, in: A. Pott, T. Bruckmann (Eds.), Cable-Driven Parallel Robots, Springer International Publishing, 2019, pp. 333–344.
[34] A. Pott, Influence of pulley kinematics on cable-driven parallel robots, in: J. Lenarcic, M. Husty (Eds.), Latest Advances in Robot Kinematics, Springer Netherlands, Dordrecht, 2012, pp. 197–204.
[35] D. Surdilovic, J. Radojicic, J. Krüger, Geometric stiffness analysis of wire robots: a mechanical approach, in: T. Bruckmann, A. Pott (Eds.), Cable-Driven Parallel Robots, Springer, Berlin, Heidelberg, Germany, 2013, pp. 389–404.
[36] A. Pott, Cable-driven Parallel Robots: Theory and Application, Springer, 2018.
[37] T. Bruckmann, L. Mikelsons, T. Brandt, M. Hiller, D. Schramm, Wire robots part i: Kinematics, analysis & design, in: Parallel Manipulators, New Developments, InTech, 2008.
[38] J.-P. Merlet, Wire-driven parallel robot: open issues, in: V. Padois, P. Bidaud, O. Khatib (Eds.), Romansy 19–Robot Design, Dynamics and Control, Springer Vienna, 2013, pp. 3–10.
[39] T. Bruckmann, A. Pott, M. Hiller, Calculating force distributions for redundantly actuated tendon-based stewart platforms, in: J. Lennarčič, B. Roth (Eds.), Advances in Robot Kinematics, Springer Netherlands, Dordrecht, 2006, pp. 403–412.
[40] P. H. Borgstrom, B. L. Jordan, G. S. Sukhatme, M. A. Batalin, W. J. Kaiser, Rapid computation of optimally safe tension distributions for parallel cable-driven robots, IEEE Transactions on Robotics 25 (6) (2009) 1271–1281.
[41] J. P. Merlet, Jacobian, Manipulability, Condition Number, and Accuracy of Parallel Robots, Journal of Mechanical Design 128 (1) (2005) 199–206.
[42] S. Kawamura, W. Choe, S. Tanaka, H. Kino, Development of an ultrahigh speed robot falcon using parallel wire drive systems, Journal of the Robotics Society of Japan 15 (1) (1997) 82–89.